Monitored Performance of the First Energy+ Autonomous Building in Dubai

G. Franchini*, G. Brumana, A. Perdichizzi

Department of Engineering and Applied Sciences, University of Bergamo, 5 Marconi Street, Dalmine 24044, Italy

Abstract

This work presents the measured performance data related to the very-first Energy+ building in Dubai certified by the Passive House Institute. The building is a two-floor office structure, with 550 m^2 total surface, designed under the guide and the scientific supervision of a Bergamo University research group, jointly to the Mohammed Bin Rashid Space Centre (MBRSC). The goal of the project was to assure a high level of internal comfort all over the year by using only solar energy. The building architecture has been designed to minimize the cooling load and the energy demand. The energy system is based on a 40 kW_p PV field coupled with a 48 kWh electric storage and a high-efficiency chiller (reversible heat pump). Transient simulations by Trnsys code have been carried out to optimize both the thermal envelope and the energy plants so to make the building energy-autonomous 24/7. The numerical predictions of the energy performance (including cooling load, PV production and power consumption for chiller, lighting and appliances) are compared to the real data measured by a sophisticated monitoring system, including sensors located in the roof, in the external walls and in the energy systems. The field measurements confirm that the model predictions were accurate both in terms of peak and annual values. The small variations between prediction and real data show that both thermal envelope and PV field perform better than expected.

This building is a pioneering pilot-project: the goal was to show that new sustainable construction standards using only solar energy are possible in the United Arab Emirates (UAE) and that this is a viable solution to reduce the carbon footprint in all the Gulf region. The strategic importance of an accurate modeling activity leading to an optimal design has been proved. The monitored data under real operating conditions have confirmed that the expected targets in terms of energy savings and carbon footprint reduction have been successfully achieved.

Keywords: Energy+ building; solar cooling; PV; monitoring system; dynamic simulation.

Nomenclature

A/C	Air conditioning system	*PPD*	Predicted Percentage of Dissatisfied
AHU	Air handling unit	*PV*	Photovoltaic
COP	Coefficient of performance	*RMSE*	Root Mean Square Error

* Corresponding author. Tel.: +39 035 2052078; fax: +39 035 2052077.
E-mail address: giuseppe.franchini@unibg.it.

DHW	Domestic hot water	*TPO*	Thermoplastic olefin
EPS	Expanded Polystyrene	U_{roof}	Roof U-value (W/m^2 K)
$g_{-value,w}$	Windows solar factor (%/100)	$U_{-value,w}$	Windows U-value (W/m^2 K)
GHI	Global Horizontal Irradiance (kWh/m^2)	U_{wall}	Wall U-value (W/m^2 K)
HP	Heat Pump	λ	Thermal conductivity (W/m K)
HX	Heat Exchanger	μ	Vapor diffusion resistance (-)
NZEB	Net Zero Energy Building	ρ	Density (kg/m^3)
PMV	Predicted Mean Vote		

1. Introduction

The global warming and the environmental problems due to air pollution are pushing the construction sector toward radical changes in the building energy management. Energy consumption and carbon dioxide emissions are continuously increasing independently on the policies adopted [1]. The development of energy-efficient buildings has been established over the years in the regions of Northern Europe and the design principles have been analyzed in several works [2, 3]. As reported in many papers, the PassivHaus-based design method provides remarkable energy savings in temperate climates [4, 5] by improving at the same time the indoor comfort [6, 7].

In the last years, the development of passive building projects in different climates [8] has attracted the scientific interest especially in hot regions [9, 10, 11, 12]. The design procedures applied in cold climates can be adapted and implemented also in warm regions with relevant results, as documented by Friess and Rakhshan [13]: their work reports on the energy efficiency improvement for residential buildings in the area of Abu Dhabi. In the MENA (Middle East and North Africa) region, the development of sustainable buildings [14, 15] as well as the introduction of innovative construction techniques such as the use of reflective films [16] are rapidly growing.

A further step toward sustainability in the construction sector is the design of an efficient thermal envelope coupled to a cooling technology driven by renewable energy sources. Several authors, such as Nanda and Panigrahi in [17] and Ghaith and Abusitta in [18], have analyzed different solar cooling technologies available on the market. Besides the thermally driven systems (including Desiccant Evaporative Cooling and solar-powered absorption/adsorption chillers), the technology based on compression chillers coupled with photovoltaic modules and energy storage is emerging as very attractive, thanks to the strong decrease of the PV costs in the last decade [19, 20]. In addition to the economic advantages, the use of cooling systems driven by photovoltaic panels resulted as the most efficient solution for several applications [21, 22].

In recent years, the development of the so-called Net-Zero Energy buildings [23, 24, 25, 26] has been facilitated by design techniques based on simulation and optimization software. These procedures allow to predict with high level of accuracy the energy performance, thus leading to a correct sizing of all components, including storage devices. For stand-alone buildings, like the ones powered by PV systems coupled with battery packs as proposed in [27], this issue is crucial. The prediction of the energy demand must include an accurate estimation of furniture and appliances, as well illustrated in [28], where authors propose a methodology for computing their impact on the energy performance. This investigation shows that furniture and appliances in Net-Zero Energy Buildings are responsible for about 15% of the primary energy

consumption.

The development of accurate numerical models is necessary for the design of high-efficiency buildings and their air conditioning systems [29, 30]. The evaluation of internal loads requires a special attention as well. Indeed, in well-insulated buildings the role of internal loads, including electrical equipment, lighting, appliances and occupancy, may be notable [31, 32]. The comfort in the well-insulated buildings is a crucial target. Several papers propose models including the computation of comfort parameters, especially in presence of radiant heating and/or cooling systems [33, 34].

The building monitoring is a powerful tool for analyzing the energy consumption and improving the energy management [35]. Data from monitoring systems are typically used for creation of databases and building classification [36, 37, 38] and to validate the simulation codes [39, 40, 41, 42].

This paper presents an initiative that documents the new strategy for a sustainable development promoted by the government of Dubai (UAE) in a long-term vision [43, 44, 45, 46]. The construction of the pioneering autonomous building in the Mohammed Bin Rashid Space Centre (MBRSC) headquarter falls in line with the UAE efforts of eliminating reliance on fossil fuels by 2050. The building, inaugurated in November 2016 and inhabited since spring 2017, is the very-first Energy+ building in Dubai certified by the Passive House Institute. Starting from a previous preliminary work on the project [47], the present paper reports the monitoring data of the first year of operation compared to the predictions.

2. Building design

The building is a two-floor office structure and it is designed to minimize the primary energy consumption. The surface to volume ratio is reduced as much as possible; all windows are sized and oriented in order to avoid direct solar gains. The wide windows overlook a small patio with a shaded garden, as shown in Fig. 1 (right).

Fig. 1: Patio with shaded garden

The external walls are prefabricated and made of different layers. The load bearing structure is built with

elements made of solid wood; walls and roof are made of timber as well. Windows, walls and roof characteristics are listed in Tab. 1 and a detailed description of the opaque elements are reported in Tab. 2 (external walls) and Tab. 3 (roof). Mass and thermal insulation thickness are specifically designed to promote the phase shift and to reduce thermal transmittance. The roof-top photovoltaic field is supported by a trimmed structure devoted to facilitate the ventilation of the PV modules and to shade the flat roof (as shown in Fig. 2). Reflective films and paints are used to minimize the solar radiation absorption on walls and roof.

Table 1. Walls, roof and windows characteristics

Wall layers		Roof		Windows	
Thickness	0.603 m	Thickness	0.566 m	$U_{\text{-value}}$	0.7 W/m^2 K
U_{wall}	0.063 W/m^2 K	U_{roof}	0.061 W/m^2 K	$g_{\text{-value}}$	0.294
Solar absorptance	0.3	Solar absorptance	0.2		

Table 2. External wall composition (from inside to outside)

Description	Thickness	Resistance μ	Conductivity λ	Density ρ	Specific Heat Capacity
	(m)	(-)	(W/m K)	(kg/m^3)	(J/kg K)
Double Plasterboard	0.025	10	0.250	800	960
Metal structure + Insulation	0.075	1	0.034	18	810
Draft-Free	0.010	1	0.067	1	1.00
Mineral Wool	0.080	1	0.034	18	810
Plaster fibreboard	0.013	19	0.350	1,200	1,000
Solid wood supporting	0.200	40	0.130	475	1,600
Mineral wool insulation	0.200	1	0.034	18	810
Reflective vapour barrier	0.0003	200,000	0.400	520	1,800
Plaster fibreboard	0.013	19	0.350	1,200	1,000
Expanse Polystyrene	0.180	30	0.037	16	1,450
Organic adhesive	0.004	240	0.900	1,700	-
Final plaster	0.003	100	0.700	1,900	1,116

Table 3. Roof composition (from inside to outside)

Description	Thickness	Resistance μ	Conductivity λ	Density ρ	Specific Heat Capacity
	(m)	(-)	(W/m K)	(kg/m^3)	(J/kg K)
Double Plasterboard	0.025	10	0.250	800	960
Solid fir wood	0.280	40	0.130	475	1,600
Mineral wool filling	0.280	1	0.034	18	810
Plaster fibreboard	0.030	200	0.13	600	2,100
Expanse Polystyrene	0.200	250	0.038	35	1,450
Sheath in TPO	0.002	150,000	0.170	1,000	1,700

The building envelope has been conceived according to the Passive House standards, as well as the energy systems have been designed to achieve the target of Energy+ Building. A 40 kW_p PV field coupled to a 48

kWh battery pack supplies power 24/7. The building is designed to operate in off-grid mode; nevertheless, the connection to the grid is operational for emergency purpose and to export the power overproduction when the energy storage is at full capacity. The A/C system is based on an air-to-water chiller, specifically designed for hot climate conditions. The chilled water is produced at different temperature levels (technical specifications are provided in Tab. 4 – right part) to drive three different cooling systems operating in the building: floor cooling, air handling unit and fan coils. The water temperature levels are controlled so to avoid uncomfortable situations. The dew point temperature of the internal air is continuously monitored, and the floor cooling water temperature is accordingly adjusted to prevent the formation of water condensate over cold surfaces. The chiller (operated as heat pump) is also providing domestic hot water.

Set-point parameters, selected to achieve a PassivHaus comfort level, and thermal gains are reported in Tab. 4 – left part. Although the design air temperature set point was 24 °C, accordingly with the PassivHaus standard, it has to be pointed out that most of the time the building has been operated with a set point of 22 °C.

The schematic of the energy system including PV cells, battery pack, appliances, chiller and air handling unit, is reported in Fig. 3.

Table 4. Set-points

Comfort & Gains	unit	value
Temperature set points	°C	22-24
Relative humidity set point	%	50
Mean ventilation ratio	ACH	0.60
HX effectiveness	%	89
Infiltration	ACH	0.06
Lighting (peak)	W/m^2	5
Internal gains (peak)	kW	6
Occupancy	Nr.	20

Cooling Equipment	unit	value
Chilled water	°C	7
DHW	°C	50
AHU water inlet temp	°C	7
Fan coils inlet temp	°C	7
Floor cooling inlet temp	°C	20
Floor temp (desired)	°C	22
Floor cooling mass flow	kg/h m^2	10

Fig. 2: Trimmed structure for the roof-top PV field

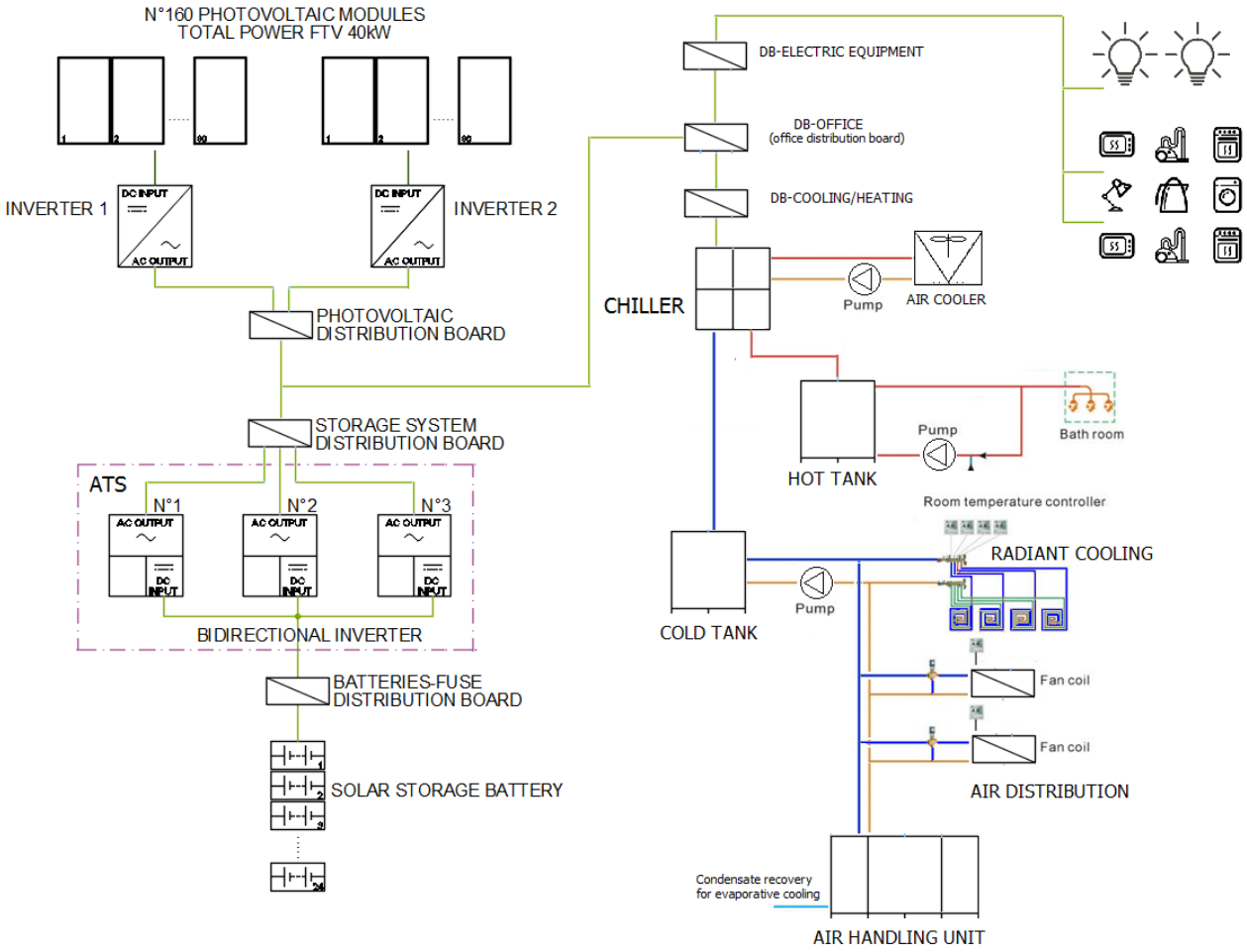

Fig. 3: Scheme of the energy plant

3. Model of thermal envelope and energy systems

A scientific approach has been followed for the building design. A model based on Trnsys17® platform has been developed both for the building envelope and the energy systems. The architectural model has been created using the 3D software Google SketchUp® coupled to the plug-in Trnsys3D. The real geometry of the building is reproduced in the 3D model (see Fig. 4), in order to predict the solar irradiation on all surfaces (walls, roof, windows) with high accuracy and to evaluate the shading effects. The model considers the internal loads, by evaluating the power consumption due to lights, appliances and the occupancy. At this regard, the number of occupants in each room, the scheduling of their presence and their activity are estimated by including some exceptional loads (for example, high occupancy in the meeting rooms for special events): the goal is to predict the cooling loads (trend and peak values) under real operating conditions. Weather data (ambient temperature, air humidity, solar irradiance) for the simulations are from the local meteo station at the Mohammed Bin Rashid Space Center headquarter.

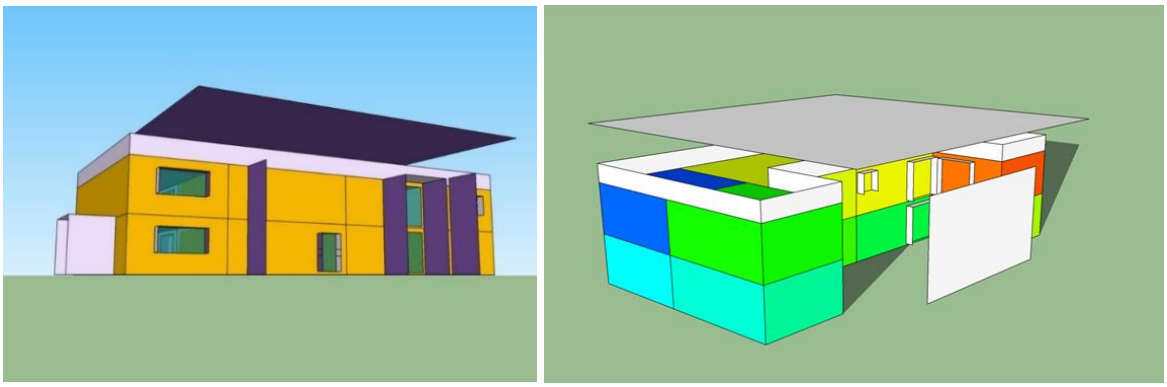

Fig. 4: Trnsys3D model

The computer model allowed to compare different building geometries, different building orientations, different wall layers and windows. The Table 5 resumes the cooling load estimation for the final configuration. The left part reports the peak load calculation for the floor cooling system and for the air-cooling system (including AHU and fan coils). On the right, the annual cooling loads are shown. For the air-cooling system, both the sensible (temperature control) and the latent (humidity control) contributions are reported. It is evident that the latent loads are dominant, because of the high level of outdoor humidity.

Table 5. Prediction of building cooling loads

Peak Load		Annual Load	
Floor cooling	7.51 kW	Floor cooling	11,741 kWh
Air cooling - sensible	5.24 kW	Air cooling - sensible	6,424 kWh
Air cooling - latent	20.30 kW	Air cooling - latent	23,201 kWh
Global peak load	26.76 kW	Total Load	41,369 kWh

In addition to the model of the building thermal envelope, a Trnsys deck for simulating the power plant and the A/C system has been developed. All electric users are powered by a field of polycrystalline photovoltaic modules (total area 268 m^2, efficiency 14.9% at standard conditions) coupled to a battery pack of 48 kWh storage capacity (technical specifications are reported in Tab. 6). The main user is the chiller (with rated cooling capacity 27.5 kW and power consumption 11.5 kW at full load). The Trnsys model includes the air-cooled chiller performance maps provided by the manufacturer (Climaveneta). Figure 5 reports cooling capacity and coefficient of performance at nominal and part load conditions, for variable ambient temperature levels. The chiller is designed to operate with an outdoor temperature up to 50 °C and the cooling capacity was selected to fulfill the peak demand of the building. All technical specifications of PV and chiller are reported in the previous work [47]. The Trnsys model of the PV field considers the air temperature effect on solar panel efficiency: this is crucial, since the PV modules operate for most of the time in very hot climate conditions.

Table 6. Energy systems' specifications

PV field and Battery specifications		
	unit	value
Area	m^2	268
Nominal efficiency	-	0.149
Efficiency modif. Temp.	1/°C	-0.0041
P_{max} Voltage	V	30.5
Open circuit voltage	V	37.6
Battery capacity	kWh	48

Heat Pump Data		
	unit	value
Chiller capacity*	kW	21.70
COP*	-	2.94
Power input*	kW	7.38
Tank Specifications		
Cold tank volume	m^3	1.00
Tank insulation (EPS)	m	0.20
Hot tank volume	m^3	0.30
Tank insulation (EPS)	m	0.20

* Ambient temperature 30 deg. C; chilled water 7-12 deg. C; load 100%

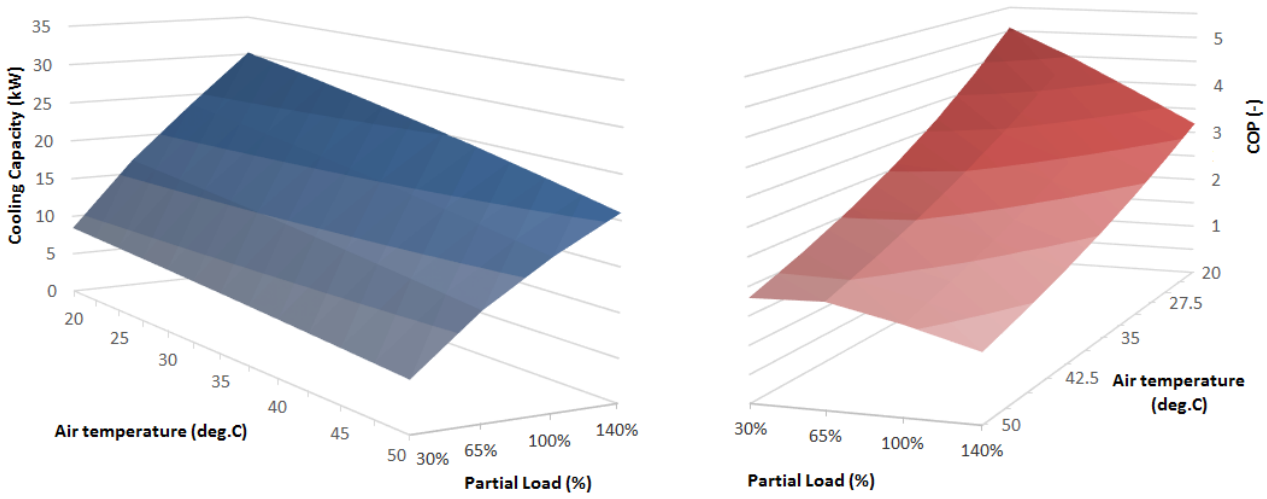

Fig. 5: Chiller performance maps

The Trnsys model reproduces the real scheme of the power system, including the control mode: the PV production gives priority to driving the local users (lighting, appliances and chiller). The overproduction is used to charge the battery pack. If the energy storage is full, the residual electricity is delivered to the grid. The results of the energy system simulations based on 1-year period are listed in Tab. 7. The constraint of energy autonomy (no import from the grid) leads to a significant overproduction of the PV field (+87%) in comparison with the total power demand. The chiller accounts for about 45% of the total power consumption.

Table 7. Prediction of energy production and consumption

Energy production	
PV production	57,734 kWh
Grid import	0 kWh
Grid export	26,916 kWh

Energy consumption	
Chiller	13,798 kWh
Light and Appliances	17,020 kWh
Total electric load	30,818 kWh

4. Monitoring system

The building is equipped with remote monitoring devices. The system includes a multitude of sensors able to measure the energy performance and the comfort level in each room. A list of the parameters monitored is shown in Table 8. The remote system operates in real time: it allows monitoring wall and roof temperatures

(external and internal side), flow rate and temperatures in every section of the AHUs (air and water side), power production and power consumption, including the battery level. All energy fluxes in the building are monitored and recorded. A web-based app makes these data available just in time (see Fig. 6).

When the building started to be used, the data monitoring permitted to optimize the control of all energy systems and to validate the numerical models. Now, the recorded data are used to check the building performance under real operating conditions.

The monitoring system works on a 3g/4g platform and a stream of information is provided from the sensors to the control room (accessible remotely). The monitoring system was developed by Wolf® System and it is based on HDL® KNX bus. The sampling time resolution is 1 minute, and the monitored data are stored directly on a server. An additional monitoring system is dedicated to the PV and battery system. This monitoring system, based on a Fronius com card, monitors the PV production, the battery parameters and the grid balance.

Table 8: Monitoring system

Weather	**PV Field & Grid**
Ambient temperature	PV production
Ambient Humidity	Grid Import/Export
Wind Velocity & Direction	Battery level
Solar Radiation	Energy balance
Building Envelope	**A/C system**
Wall temperatures (int/ext)	Cooling production
Roof temperatures (int/ext)	Chiller power consumption
Floor temperatures	AHU in/out temperatures
Comfort	Floor cooling in/out temp.
Air temperature	Storage temperature
Humidity	Water Flow rates
CO_2	**Thermal Loads**
Air velocity	Lighting consumption
Luminosity	Appliance consumption

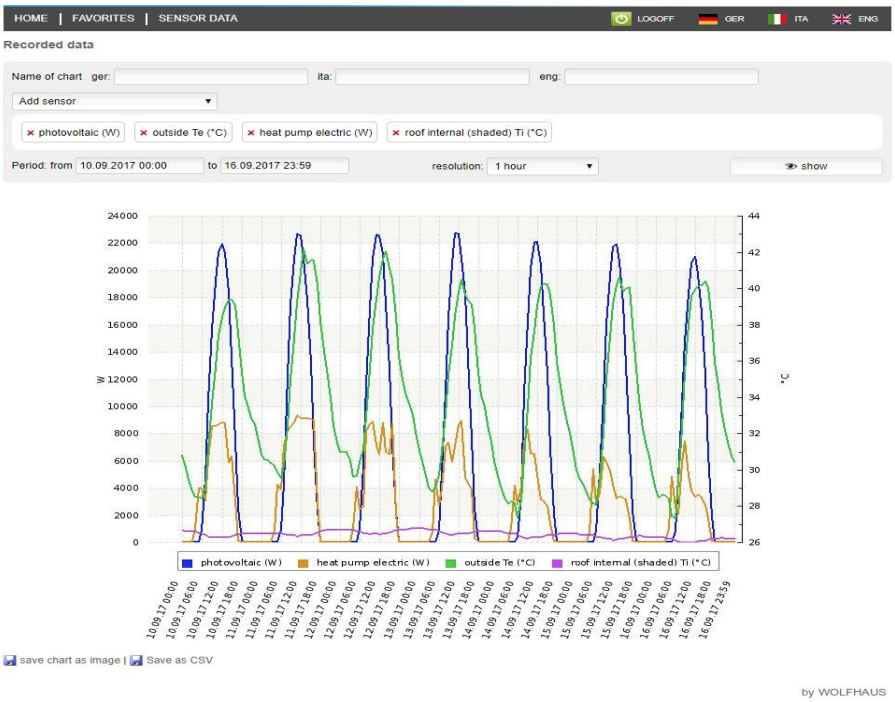

Fig. 6: Screenshot of the monitoring web-based app (developed by Wolfhaus)

5. Comparison model prediction vs. monitoring data

The data collected by the sensors have been compared to the results of the numerical models. The goal is to check the quality of the design procedure based on Trnsys simulations. The comparison has been carried out for operative parameters of both the building envelope and the energy systems. The period considered covers one year, from when the building was used as office building. The graphs in the following paragraphs show real and predicted data for a 4-day period in summer (July 2017) and winter (February 2017), in order to evaluate if the model can predict with accuracy the hourly variations. In order to compare properly the model predictions (originally performed with Meteonorm weather data in the design phase) and the real data, a new set of simulations have been carried out, by including the real meteorological data in the model. The curves presented in the following charts as "model" refers to the prediction with the real weather data.

5.1 Thermal envelope

Figures 7a and 7b show the cooling load according to the model prediction (dotted lines) and the real data (solid lines) in 4 consecutive days of July and February respectively. Measurements and simulation results show a good superposition for both the seasons, with a moderate overprediction, mainly in the summer mornings. This is due to the control strategy for the summer period: after sunset, the floor cooling system switches on with a nighttime set-point. So, the massive layers remain cool till the next morning. This system performs better than the prediction, by lowering the cooling loads in the first hours of the day.

In winter the floor cooling is off nighttime. The peak load at early morning is accurately predicted by the model.

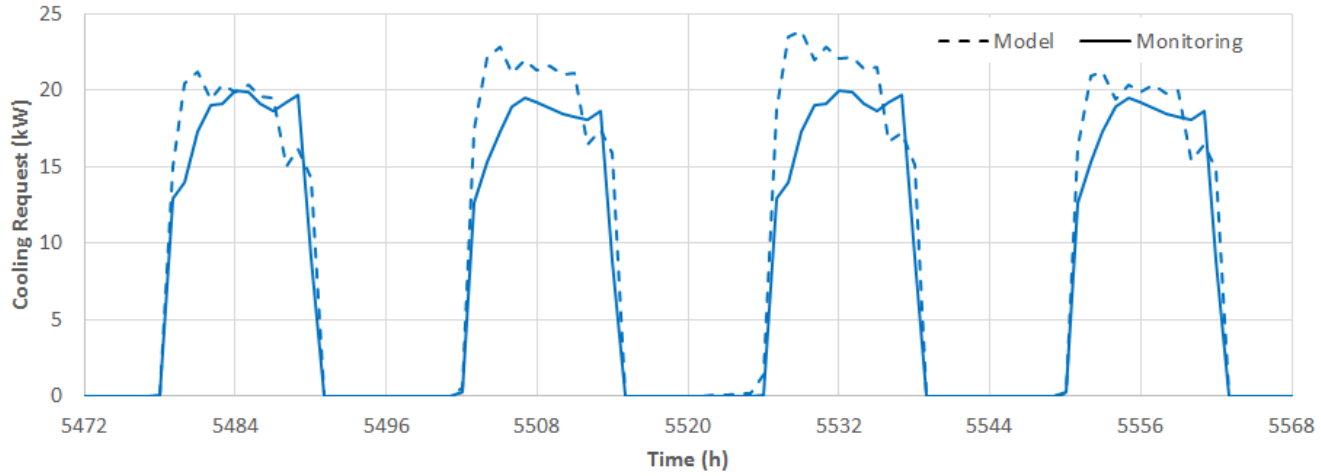

Fig. 7a: Cooling load (July)

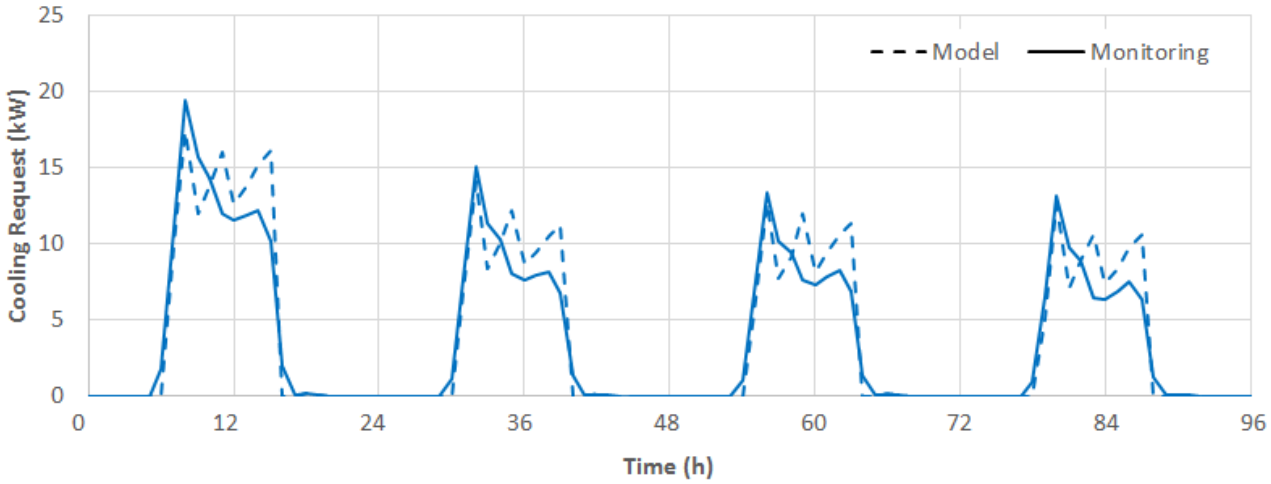

Fig. 7b: Cooling load (February)

Figures 8a and 8b show the internal air temperature trend in the open workspace on the ground floor during the 4-day period in July and in February respectively. In the same chart, the outdoor temperature is reported as well. The analysis of the curves shows a very good superposition between model and measurements.

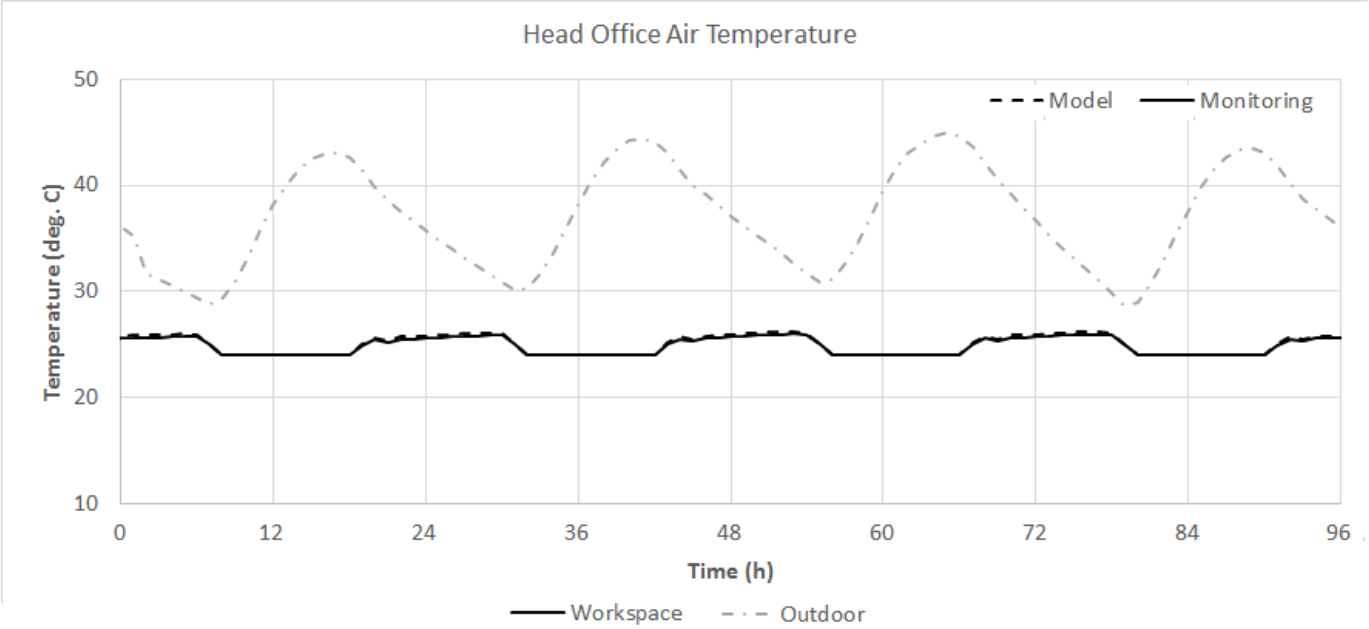

Fig. 8a: Air temperature in the open workspace (July)

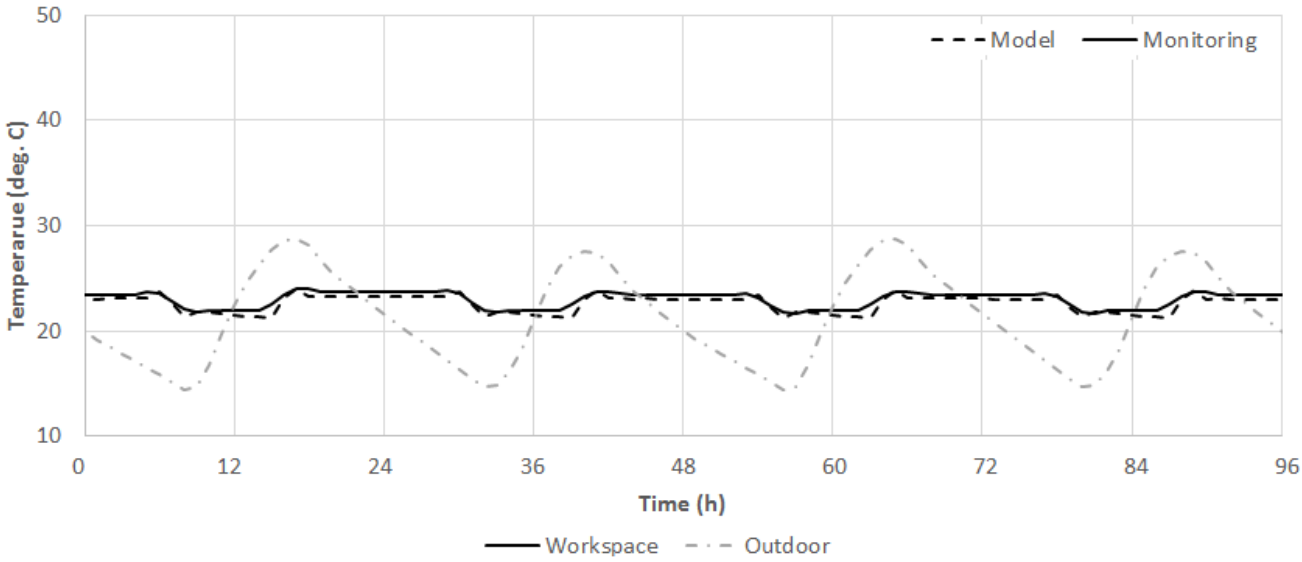

Fig. 8b: Air temperature in the open workspace (February)

Moving to the solid walls, Fig. 9a and Fig. 9b show the trend of the internal and external temperatures of the west-facing wall, while Fig. 10a and Fig. 10b those of the flat roof. The numerical model exhibits a very good capability to predict the temperature levels measured by the thermocouples. In July the external side of the west-oriented vertical wall reaches a temperature of 50 °C, whilst the internal side remains under 24 °C. Due to the orientation, the external wall temperature increases with a time shift with respect to the ambient temperature in the morning, while in the afternoon the wall temperature remains 2-3 °C higher because of the solar irradiance.

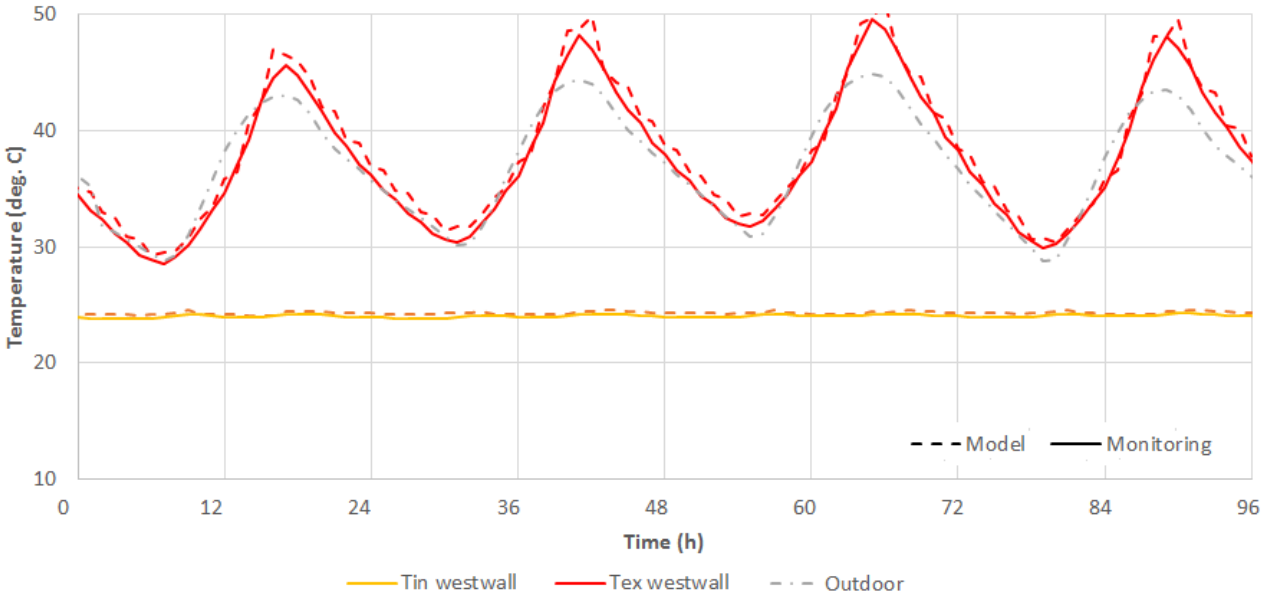

248
249

Fig. 9a: West-facing wall temperature (July)

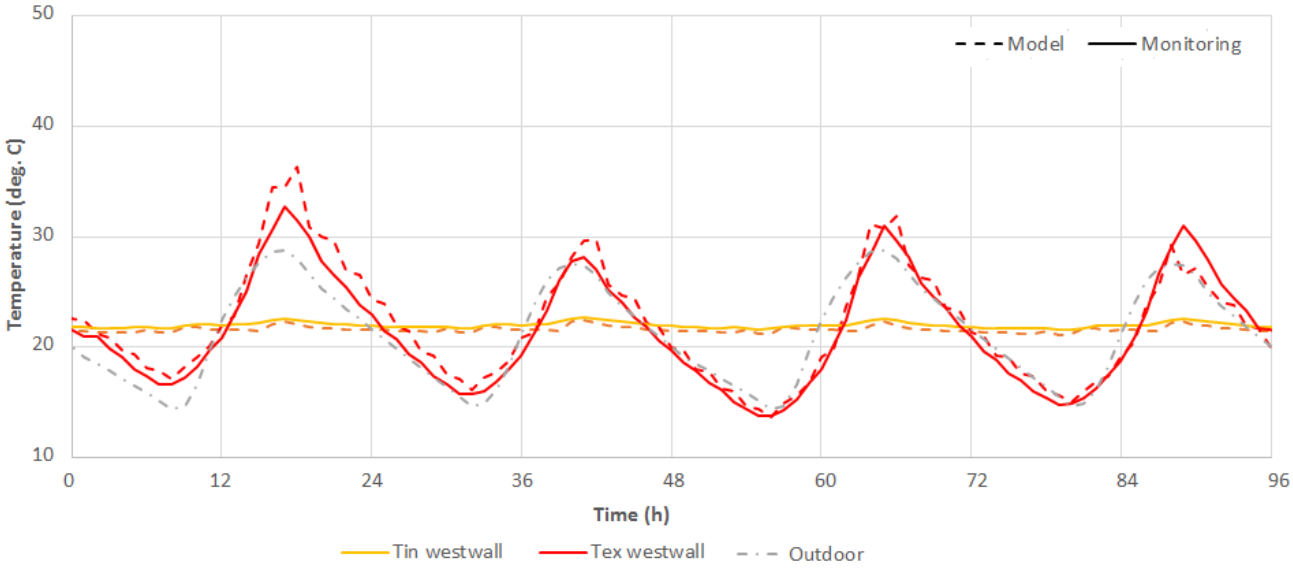

250
251

Fig. 9b: West-facing wall temperature (February)

252

253 The roof temperature undergoes a steep increase since the early morning due to solar radiation. The good
254 insulation of the roof is testified by the constant temperature at the internal side (25 °C), while the external
255 temperature oscillates between 28 and 48 °C.

256

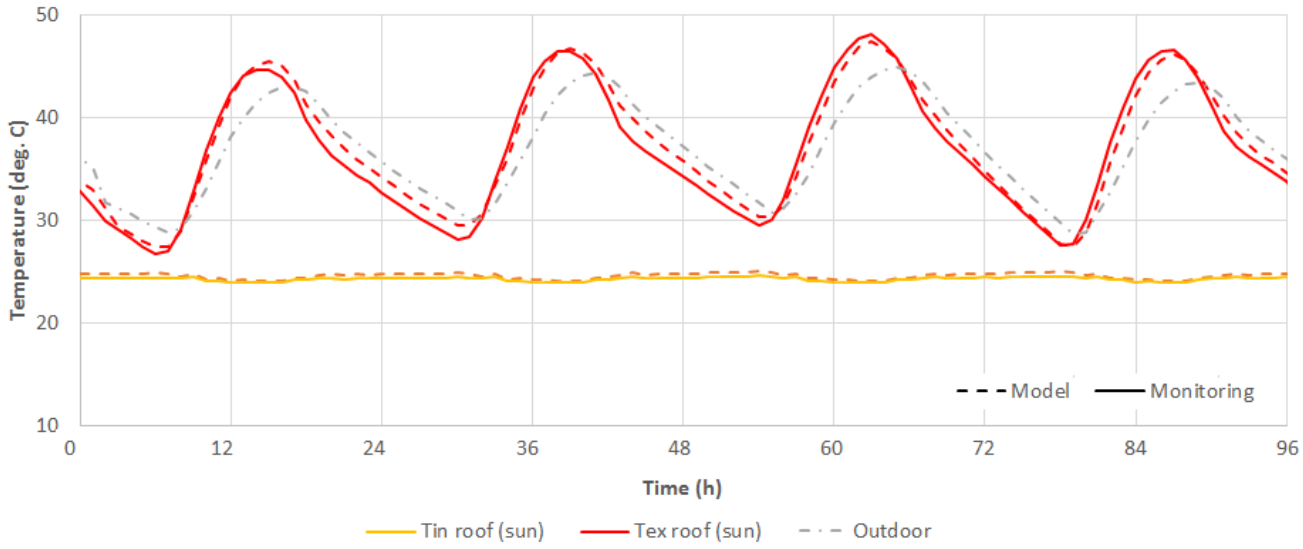

Fig. 10a: Roof temperature (July)

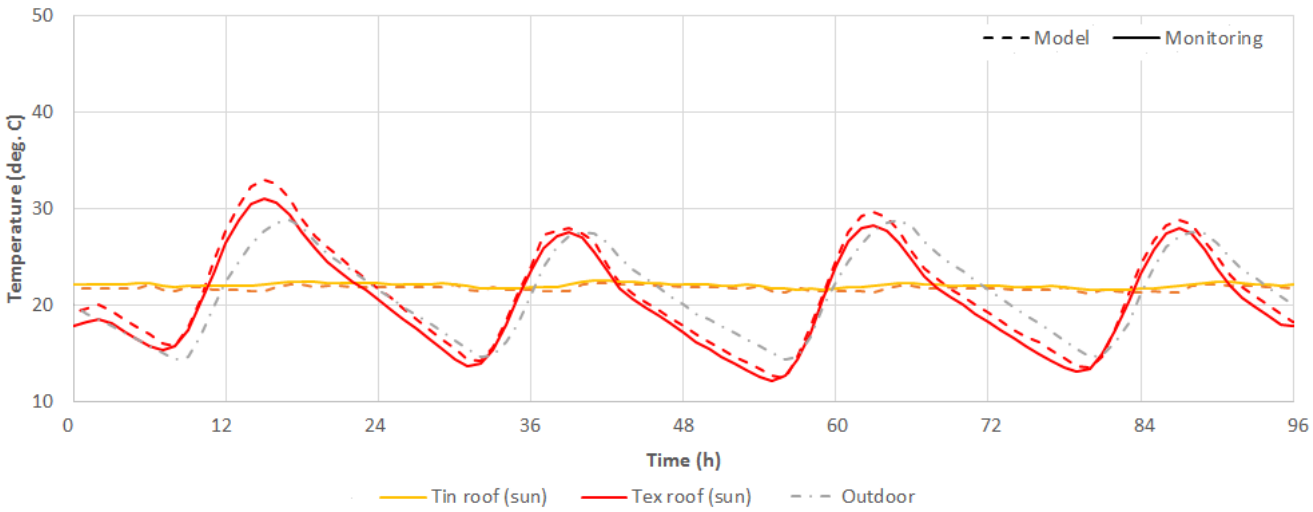

Fig. 10b: Roof temperature (February)

The combination of cooling technologies and a proactive control strategy of the energy systems leads to a very good internal comfort despite of the critical outdoor conditions. Figure 11a and Figure 11b show the Fanger's parameters evaluated with the Trnsys simulations. The predicted percentage of dissatisfied (PPD) persons reported in black shows a trend close to the minimum value (5%). The predicted mean vote (PMV), red line, shows a very high perception of comfort. The PMV results to be included in the best range (-0.5:0.5) all year long.

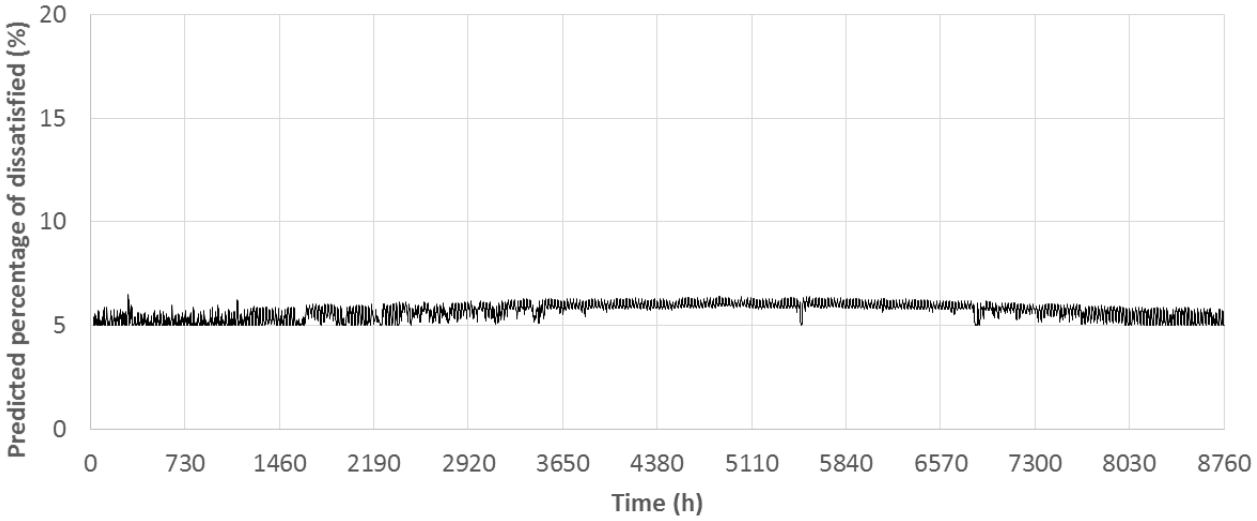

Fig. 11a: Fanger's parameter Predicted Percentage of Dissatisfied persons (PPD)

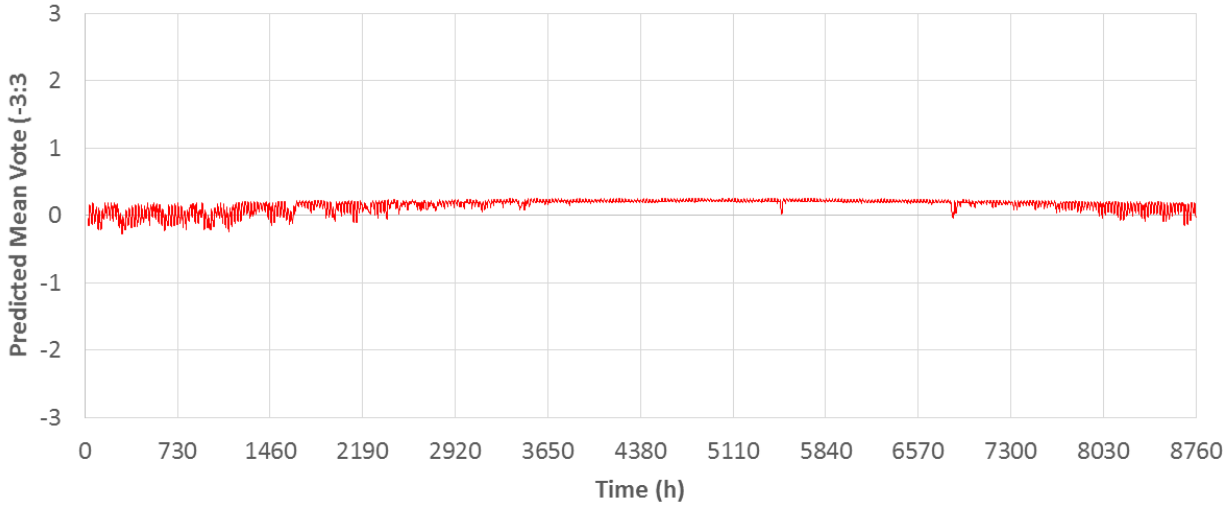

Fig. 11b: Fanger's parameter Predicted Mean Vote (PMV)

5.2 Power plant and cooling system

As mentioned in paragraph 3, the energy system including PV, batteries and A/C system is fully monitored, in order to measure the actual performance of each component. Figures 12a and 12b show the cooling production and the power consumption of the chiller in the summer and winter period respectively. The black lines report the corresponding cooling load shown in Fig. 7a and Fig 7b: the slight difference between the cooling load and the heat pump cooling production is due to the chilled water buffer tank. A general good agreement can be observed between numerical model and real data. The model prediction slightly exceeds the real cooling production and power consumption, according to the moderate overestimation of the cooling load documented in Fig. 7a and Fig. 7b. In the July period, the chiller switches on at part load during the night to keep the chilled water in the floor cooling system at the set-point. The Trnsys model predicts (with a small delay) the nighttime start-and-stop of the chiller. In Fig. 13 the chiller COP in summer and winter conditions is reported. The chart shows a good superposition between model and monitored results. The dashed lines indicate the ambient temperature and the COP correlation with

temperature is evident: the higher is the air temperature, the lower is the chiller efficiency. Moreover, the part load operation can positively influence the chiller efficiency, as documented in Fig. 5. In February, the COP is higher than 4 for several hours, thanks to the beneficial effects of the low outdoor temperature and the part load operation, due to the low cooling load.

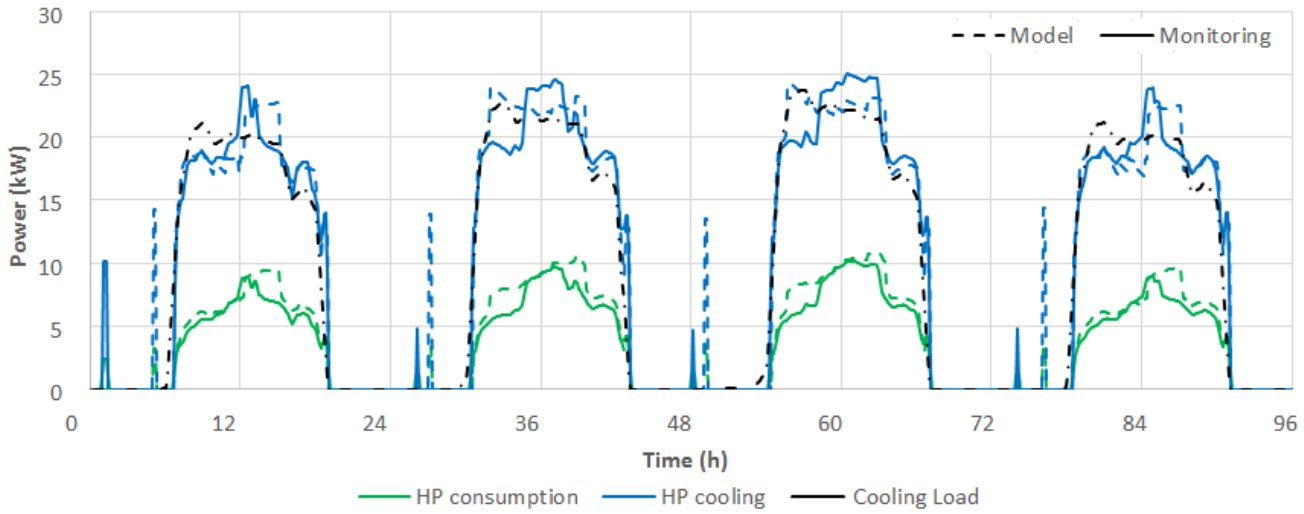

Fig. 12a: Chiller cooling production and power consumption (July)

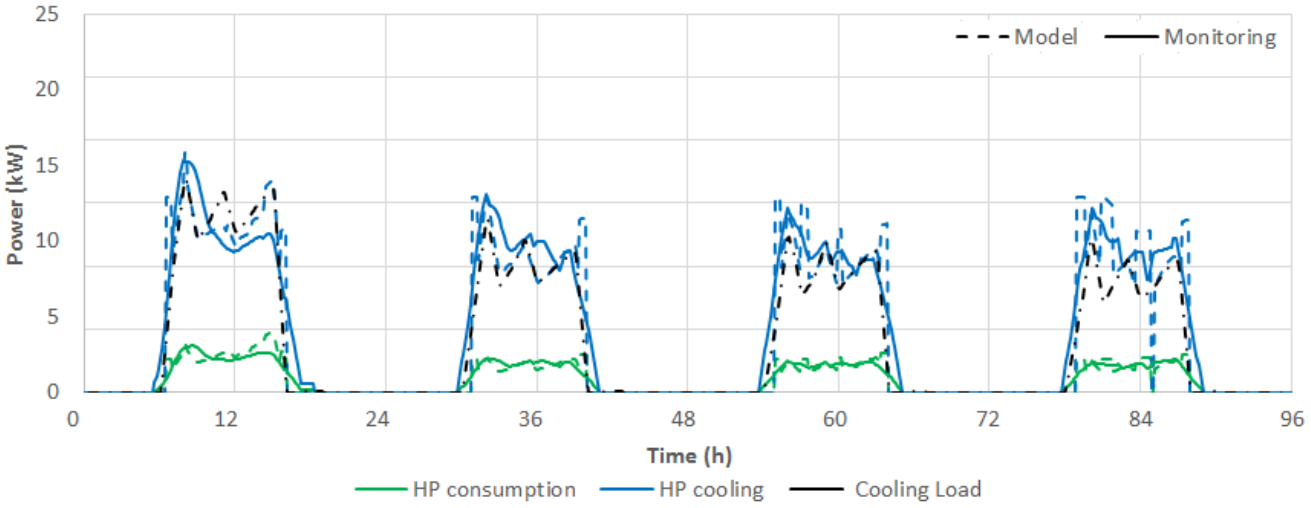

Fig. 12b: Chiller cooling production and power consumption (February)

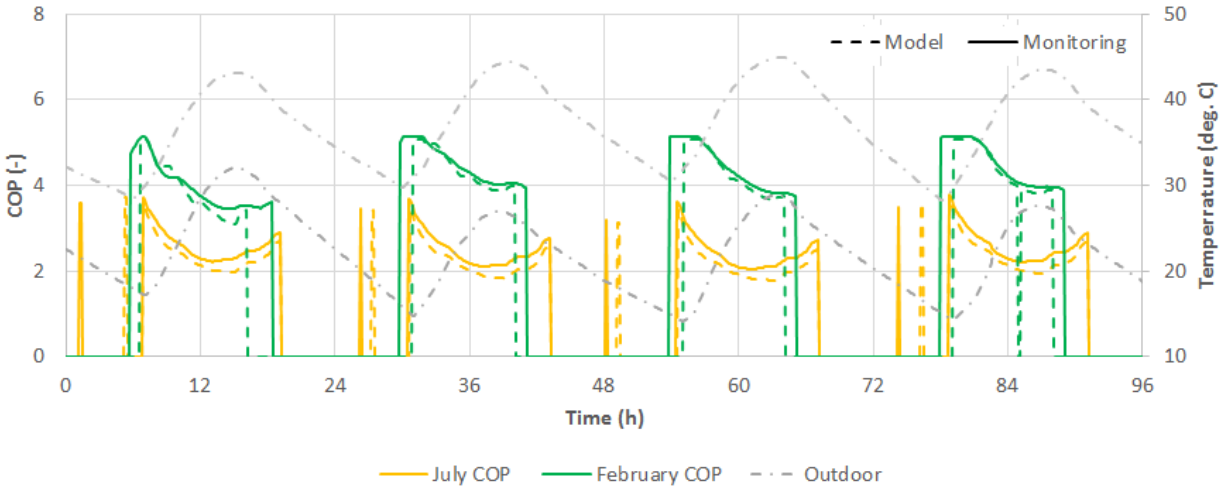

Fig. 13: Chiller COP

Moving to the power system, Fig. 14a and Fig. 14b show the PV production (violet line), the power demand of the chiller (green line) and the power consumption of lights and appliances (orange line). The power output of the PV field appears slightly underestimated by the model: this is probably due to the typical PV overproduction in the first year of operation, which is neglected by the Trnsys model. The PV peak power is higher in February than in July (28.5 kW vs. 26 kW), despite a lower solar irradiance and a higher cosine effect: the beneficial effect of a lower operating cell temperature (in winter) appears dominant. The PV model includes the temperature de-rating and the radiation de-rating functions: in summer, the cell temperature reaches a peak of 92 deg. C, whilst in in February the peak temperature is about 74 deg. C.

The power consumption of the equipment is well predicted, with a small overestimation of the chiller consumption, as already mentioned before.

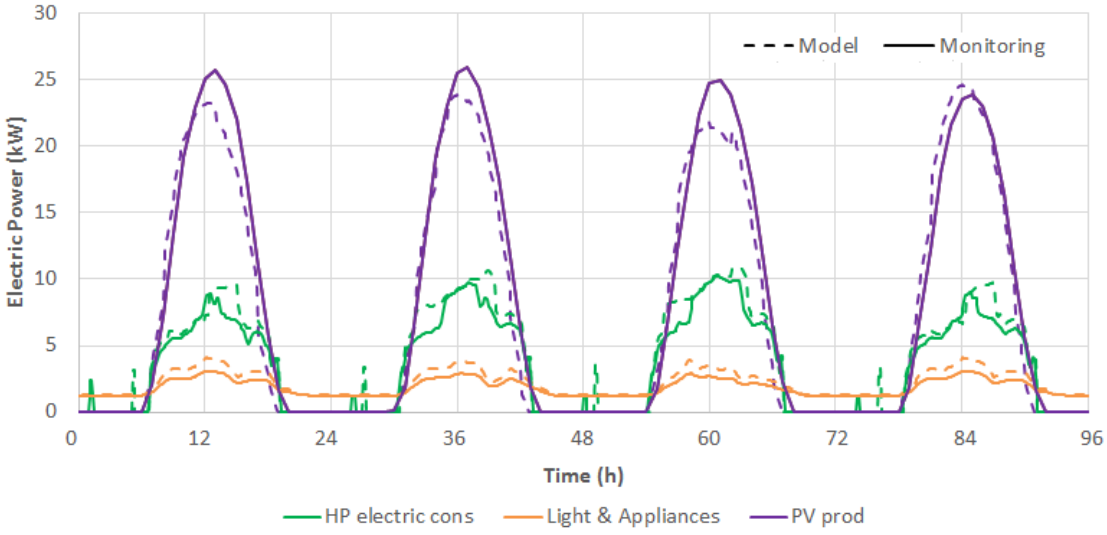

Fig. 14a: PV electric production and power consumption (July)

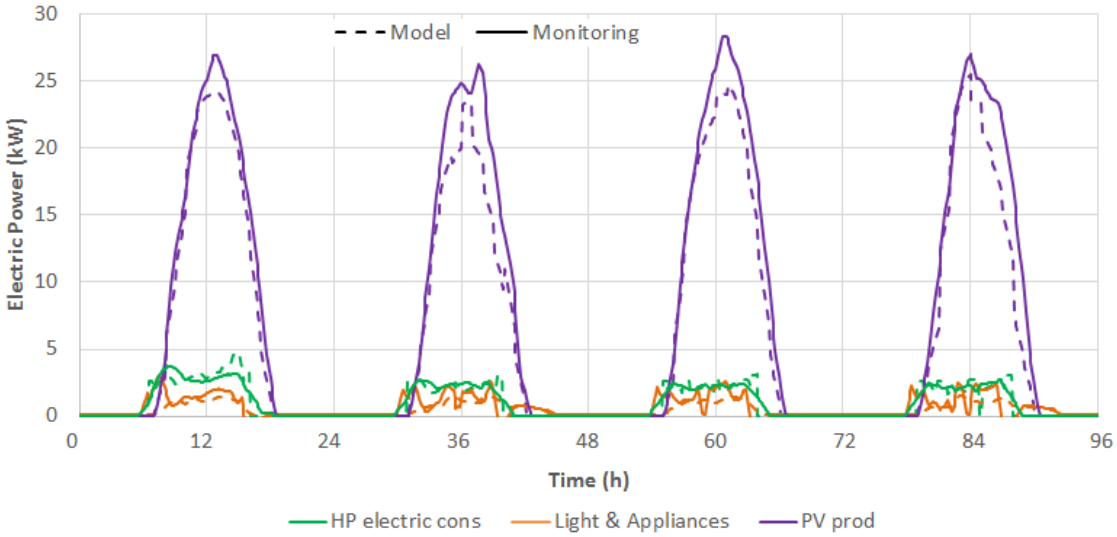

Fig. 14b: PV electric production and power consumption (February)

Moving now to the power balance of the building, the charts reported in Fig. 15a and Fig. 15b show the overall power demand of the building (red line) and the power export to the grid (black line) taking place when the battery pack is fully charged. On the same chart the PV power output (already shown in Fig. 10a and Fig. 10b) is reported (violet line) to easily compare power production and consumption. At early morning, when the air-cooling system switches on, the PV power supply covers the demand. Starting from 10 a.m. the solar production exceeds the power consumption and when the battery charge is completed, the overproduction is delivered to the grid. This occurs both in July and February because the constraint of energy autonomy forced to slightly oversize the PV field to get some margin. Looking at the PV production, the model (dotted lines) shows once again a good agreement with the measured data: a small deviation occurs at the beginning of the export times, when the model predicts an instantaneous shift from the mode “power-to-battery” to the mode “power-to-grid”, whilst the real control system starts the power export when the battery pack is not completely full-charged. This is due to the typical non-linear behavior of the battery when it is approaching the full charge condition: the Trnsys model neglects this power charge limitation.

Moreover, Fig 15a and Fig. 15b show a different behavior in the night-time operation. In the summer period, the chiller switches on once a night to keep the temperature under the night set-point level (26 °C). In February the outdoor temperature is below the set-point and the air handling unit can operate in free cooling mode.

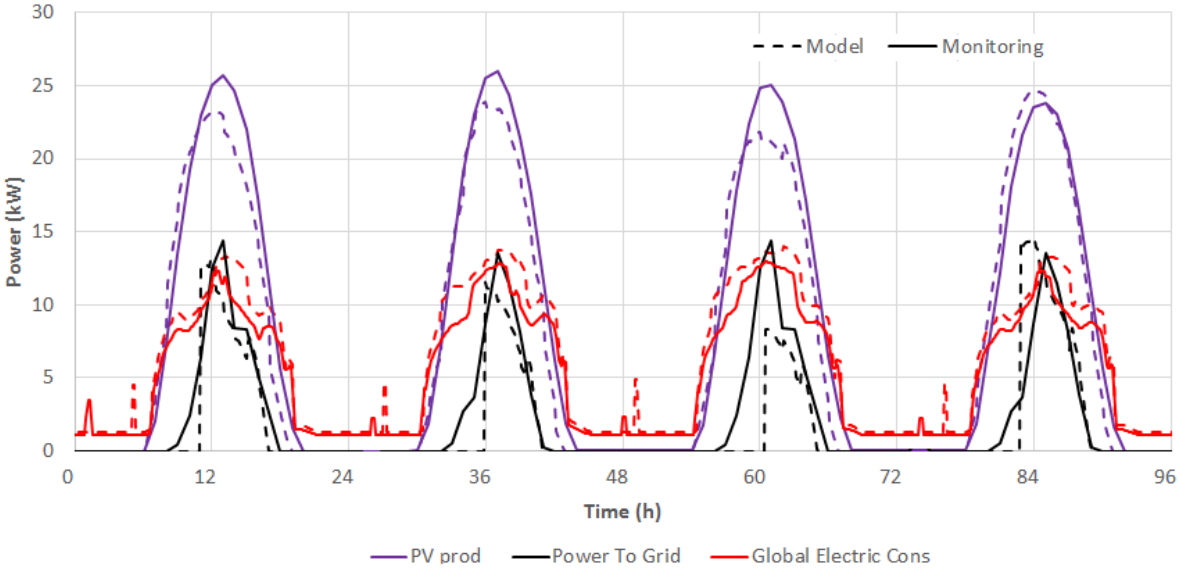

Fig. 15a: Grid analysis: power production, consumption and export (July)

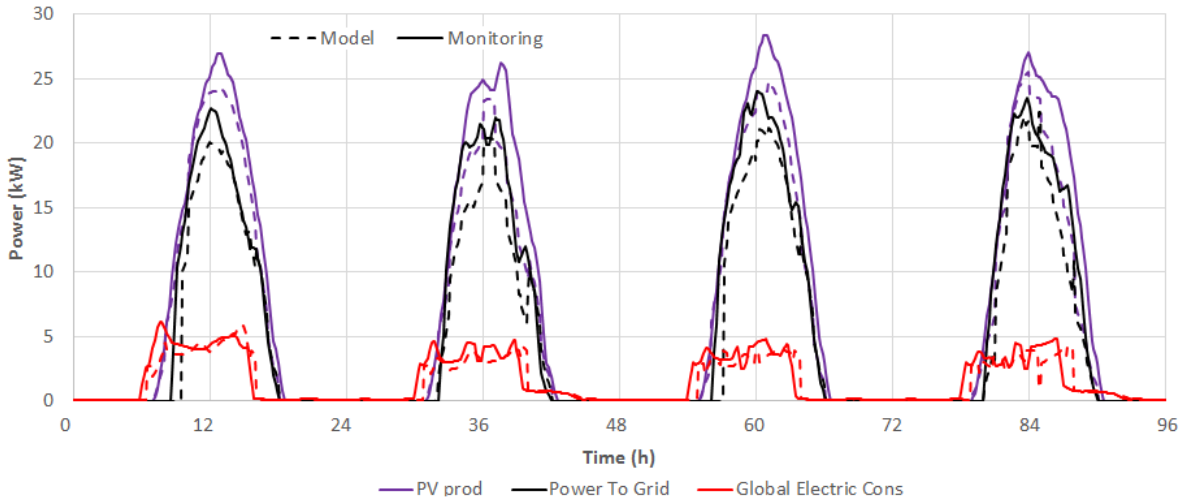

Fig. 15b: Grid analysis: power production, consumption and export (February)

Figures 16a and 16b show the battery charge level during the 4-day periods in July and February respectively. Even though the predicted values are generally lower than real data in the switch phases (i.e. from charge to discharge mode, and vice-versa), the trend is the same and it can be said that the model prediction is good. The amounts of energy exported and stored are correctly evaluated by the model. In winter, when the cooling loads are low, the battery level remains in the range 90-100% and most of the PV production is delivered to the grid. In the design phase, using the Meteonorm database the battery capacity was determined to keep the fractional state of charge at 20 % during the worst hour, occurring in a hot and cloudy day of July. With the real weather datasets, the minimum battery level resulted to be 39% in the simulation results and 56% in the monitored data.

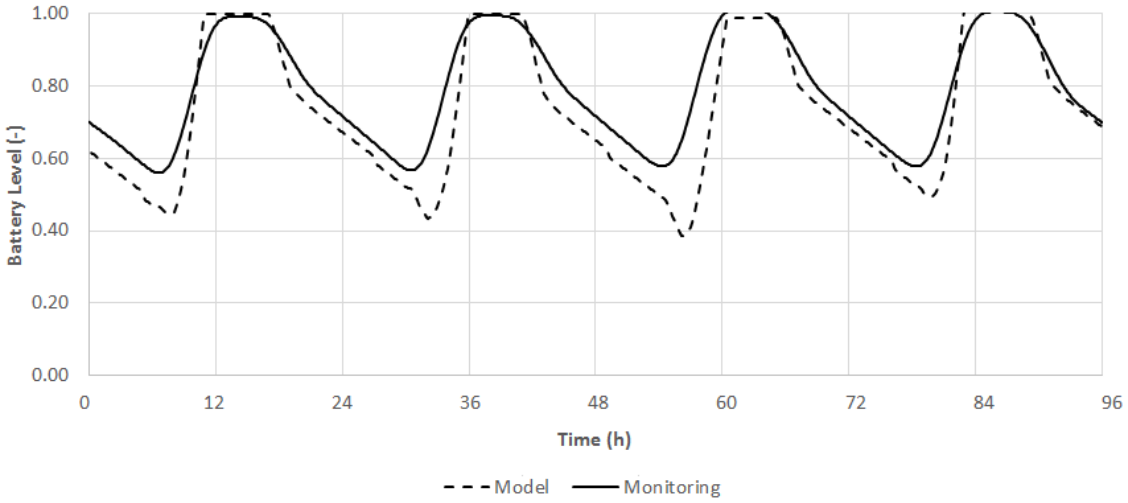

Fig. 16a: Battery level (July)

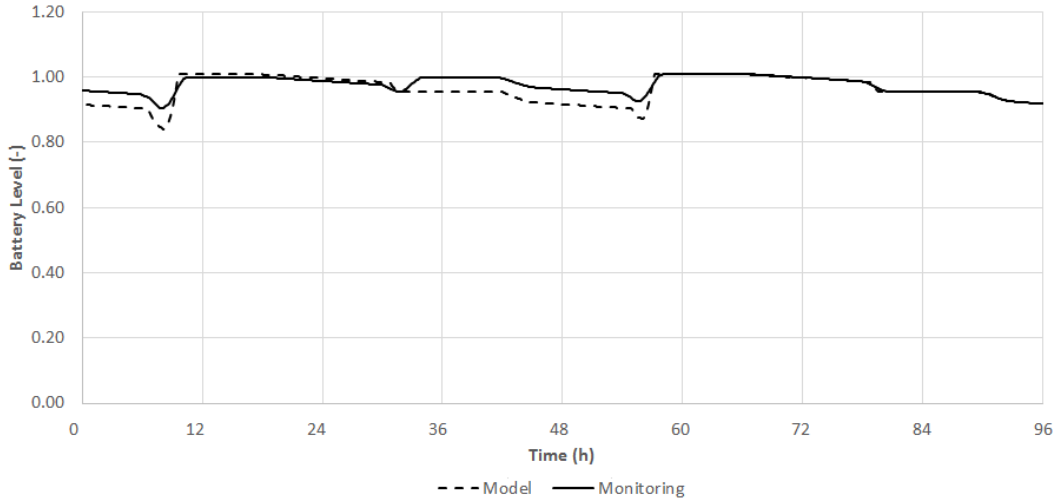

Fig. 16b: Battery level (February)

Table 9 reports the error analysis of the presented results. For the main performance parameters, the Root Mean Square Error (RMSE) is shown. The RMSE is evaluated on annual basis: the results confirm a good agreement between numerical model and monitored performance.

Table 9. Error analysis

Thermal envelope	RMSE		Energy systems	RMSE
Cooling Load (kW)	1.146		PV production (kW)	3.461
Air Temperature(deg.C)	0.293		HP consumption (kW)	0.303
Wall Temperature Tin (deg.C)	0.288		HP cooling production (kW)	0.956
Wall Temperature Tex (deg.C)	1.176		COP (-)	0.193
Roof Temperature Tin (deg.C)	0.325		Light and Appliances (kW)	0.487
Roof Temperature Tex (deg.C)	1.161		Global electric consumption (kW)	0.911
			Power to Grid (kW)	1.102
			Battery level (-)	0.329

6. Annual yield

Moving to the annual simulation results and the corresponding monitored data, the following bar charts show the monthly trends of different physical quantities: the dark color indicates the measurements, whilst the light color is used for the numerical predictions. The chart in Fig. 17 shows the monthly cooling load of the building: the model overestimates the cooling demand in the warmest months (+4% on average), whilst the prediction is more accurate in winter.

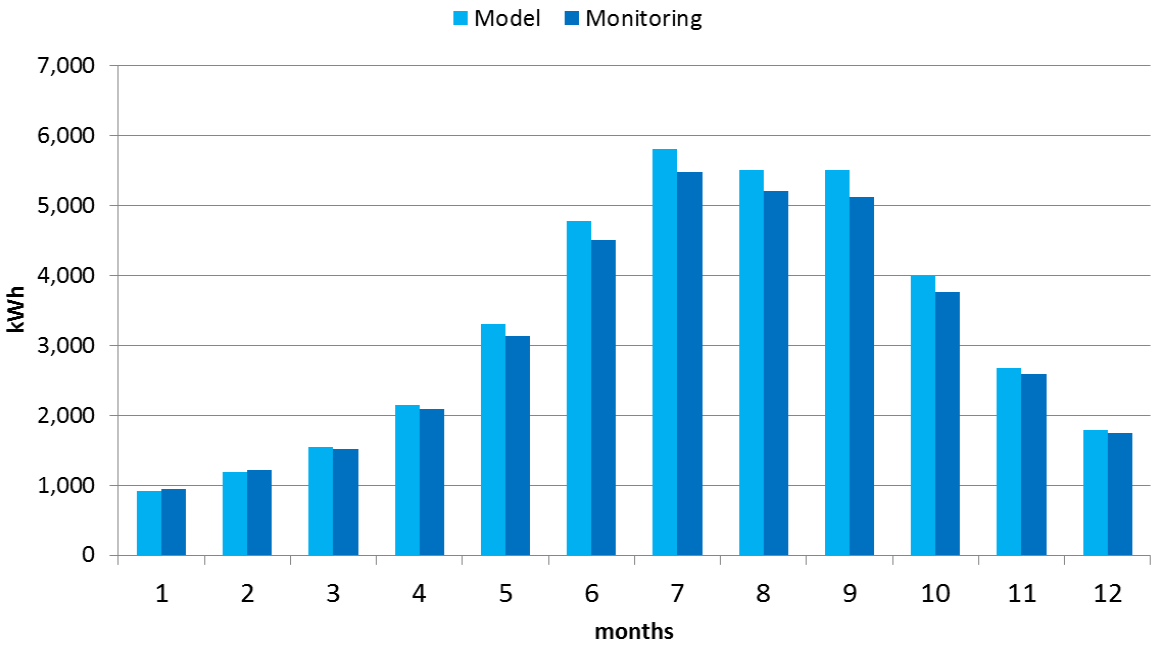

Fig. 17: Monthly cooling load

Figure 18 reports the monthly trend of the PV power production. It has to be reminded that the PV field is installed on a horizontal roof: this position favors the summer operation, when the solar zenith angle (and consequently the cosine effect) is lower. Nevertheless, the high ambient temperature has a detrimental impact on the cells' efficiency (whose monthly average values are reported in the chart): the combination of these two factors leads to a peak production in May. Being the available annual radiation on the horizontal plane (GHI) equal to 1,956 kWh/m^2, the annual average efficiency of the PV field resulted to be 11.54%. The de-rating from the design value (14.9%) due to the operating cell temperature (up to 75 °C in the summer) is 3.36 point. Comparing model vs. real data, the PV field production is higher than expected in every season (+4% on average). The power overproduction is likely to be due, as typical, to the higher efficiency of the PV modules in the first year of operation. The authors expect a PV output reduction in the next years with a consequence alignment in the electricity production. Moreover, the efficiency coefficient provided by the manufacturer and considered in the model (i.e. the multiplier to correct the rated PV cell efficiency as a function of the cell temperature) could be conservative.

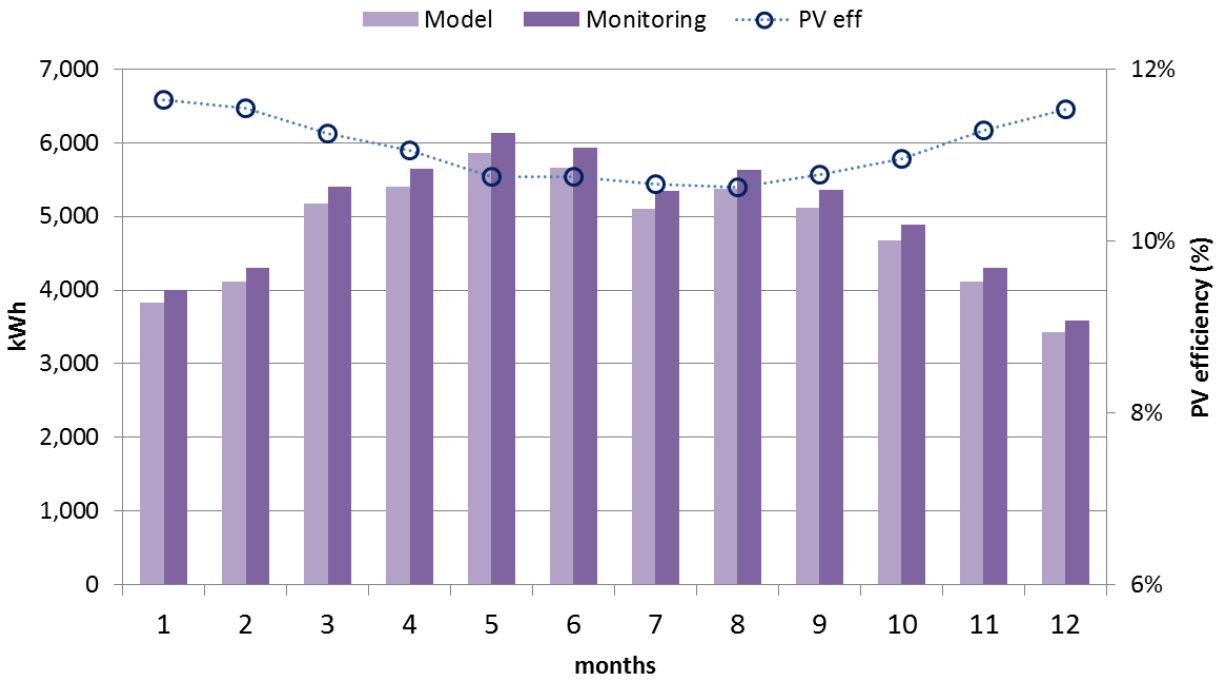

Fig. 18: Monthly PV electric production

Figure 19 shows the overall energy consumption in the building. The model predicts very well the amount of electricity demand for lighting, appliances and A/C, apart from the summer months, when the overestimation of the cooling load leads to an increased estimation of the chiller energy consumption.

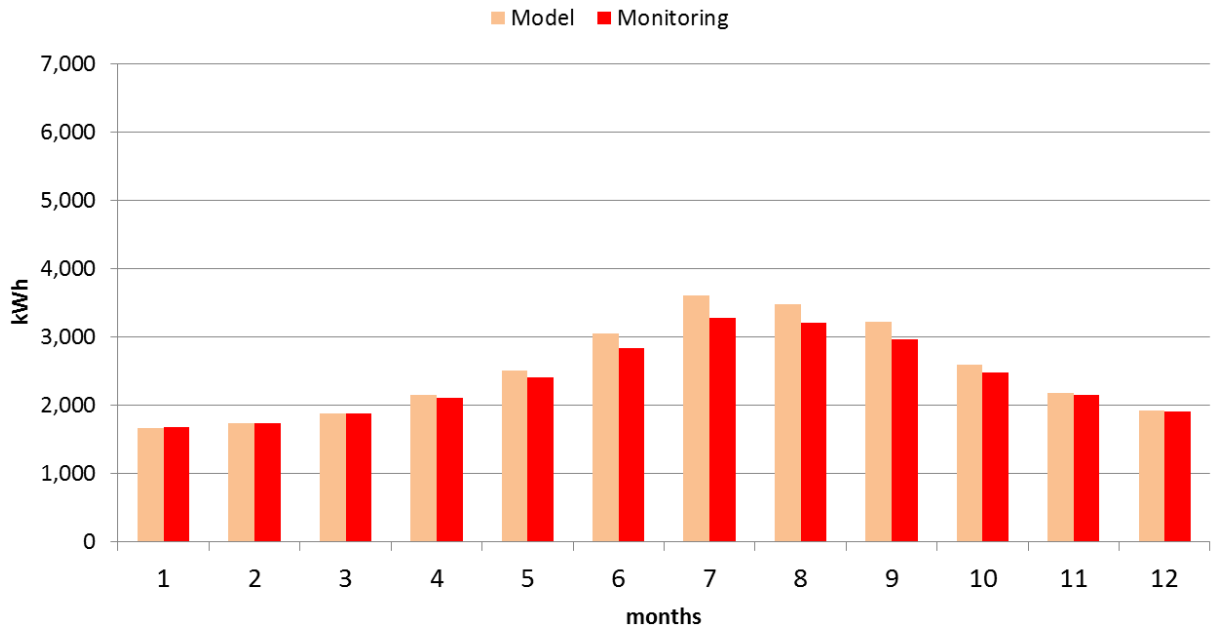

Fig. 19: Monthly electric loads

Figure 20 shows the energy balance of the building-grid system: positive values mean power export, whilst negative values would indicate power import. As it can be noted, the bars show that the target of autonomous house is achieved all year long, as the import from the grid is always zero and power export to the grid occurs

all the months. The maximum of export takes place between March and May (more than 3,500 kWh per month), when the solar irradiance and the PV output are high, while the cooling demand (and consequently the chiller power consumption) is moderate. The combination of the cooling load overestimation (+4.9%) and the PV production underestimation (-4.4%) cause a deviation in the export estimation equal to 12% with respect to the monitored data. As discussed in more detail in the next paragraph, the requirement of full energy-autonomy obliges to over-size the energy systems. The data reported in Fig. 20 confirm this issue, as the minimum export to the grid is about 1,400-1,500 kWh/month in December and July, corresponding to the periods with the lowest solar energy and the highest cooling demand respectively.

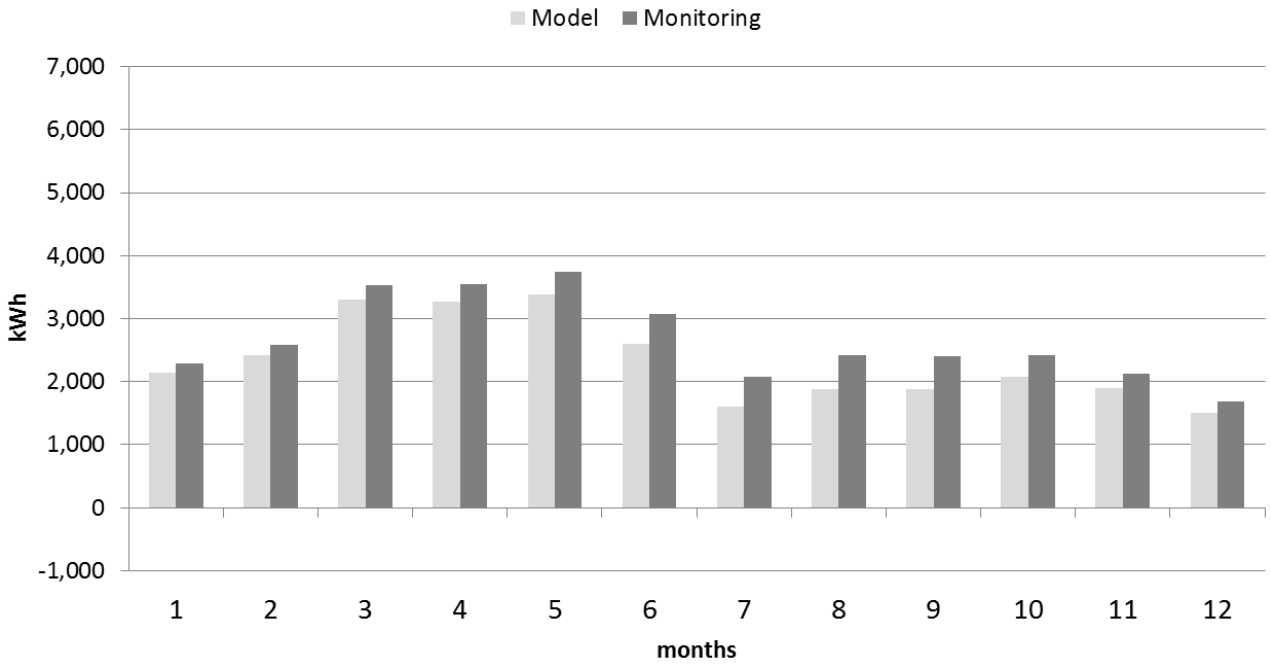

Fig. 20: Monthly energy import and export

Table 9 summarizes the annual energy balance for the building and the deviation between predictions and measured data. One can note that the 268 m^2 PV field is producing not only the energy required for the building operation, i.e. lighting, appliances and chiller consumption (28.6 MWh), but also a similar amount (31.9 MWh) exported to the grid. The large excess is mainly due to the need to satisfy the daily electricity demand even in the hottest days of the year. In other words, the system was designed to have in those days an energy balance close to zero, but always positive with some margin, so to guarantee the building requirement to be autonomous. The real data related to the building energy behavior, i.e. the cooling load, the chiller consumption and the electric load resulted all about 5% lower than the predicted values. Nevertheless, these differences shall not to be considered too large because there are different factors influencing the real building performance that cannot be predicted by any simulation model. The major ones are:

1. real occupancy and appliances are different from the assumed ones;
2. performance of installed equipment/systems are different from the nominal ones;
3. unpredictated changes of temperature set points.

As a general evaluation, it can be concluded that the accuracy of the model predictions is good and more than satisfactory.

Table 9. Annual energy balance

	unit	Measurement	Model	Deviation (%)
PV production	kWh	60,520	57,845	-4.42%
Total electric load	kWh	28,621	29,958	4.67%
Lighting and appliances	kWh	16,163	16,923	4.70%
Chiller power consumption	kWh	12,458	13,035	4.63%
Cooling Load	kWh	37,310	39,148	4.93%
Cooling production	kWh	37,554	39,310	4.68%
Specific annual consumption	kWh/(m^2a)	67.8	71.2	4.93%
Import	kWh	0	0	0.00%
Export	kWh	31,899	27,887	-12.58%

7. Techno-Economic evaluation of the off-grid requirement

The full energy-autonomy of a building in a desert region is an intriguing target. To do that, the power generation and energy storage systems must be large enough to avoid any import of electricity during the year, including the periods of peak demand. Evaluating how much a PV field must be oversized to meet the off-grid requirement of an office building in the Dubai area is one of the goals of the prototype presented in the paper. In order to calculate the extra-size and the extra-costs of the autonomous configuration, three alternative cases, representing three different standards, have been considered: 1) a traditional on-grid building; 2) a Net Zero Energy Building (NZEB); 3) a NZEB with storage system. The configuration 1 is the reference case of a traditional building without PV panels nor storage devices, importing power from the grid. In the NZEB case, the import and export of electricity are balanced on annual basis. The size of the PV field was determined in an iterative way. The case 3 exhibits the same PV area of the case 2 (NZEB) and the same storage capacity of the autonomous building. For each configuration, annual simulations have been carried out under the same weather conditions (measured data) of the off-grid building case. Table 10 reports the simulation results of the four cases. The electricity bill has been calculated according to the monthly import and export amounts and the current rules established by the local energy authority. The electricity cost is 0.2950 AED/kWh from 0 to 2,000 kWh/month and 0.345 AED/kWh over 2,000 kWh/month. The power to the grid is refunded 0.230 AED/kWh. The conversion rate is 3.6725 AED/USD. For the economic and environmental analysis, the surplus of electricity is supposed to be sold to the grid (or to the neighboring buildings) for the off-grid configuration; otherwise, the surplus must be dissipated, according to the operation in island mode.

Comparing the solar field areas, moving from the NZEB standard to the off-grid requirement (case 2 vs. case 4) the required PV surface undergoes a relevant increase (+87%). The extra-cost for the PV field is almost 28,000 USD, and the cost of the battery pack is about 25,000 USD.

Looking at the grid balance, the off-grid case, as mentioned before, exhibits a huge surplus (93% of the total electricity demand). In the NZEB case, the grid exchange amounts to about 33% (9.8 MWh). The use of a 48 kWh storage system allows to reduce to less than 10% (2.9 MWh) the grid exchange.

As a general comment, the very low cost of electricity in the Dubai region makes the traditional on-grid

configuration the most cost-competitive. Nevertheless, the economic profitability is not always the primary target. The aim of the present project, promoted by the Government of Dubai, includes a sustainability challenge. With a 33.9% average efficiency of the power sector [48] and an estimated 0.50 kgCO_2/kWh emission factor, the building in the off-grid configuration permits a CO_2 emission reduction of 28,950 kg/year.

Table 10. Comparative analysis of different standards

		1. No PV	2. NZEB	3. NZEB w/ storage	4. Off-grid
Solar field & Storage					
PV area	m^2	0	143	143	268
Battery pack	kWh	0	0	48	48
Annual yield					
PV production	MWh	0	30.0	30.0	57.8
Electric consumption	MWh	30.0	30.0	30.0	30.0
Import	MWh	30.0	9.8	2.9	0
Export	MWh	0	9.8	2.9	27.9 (*)
Costs					
PV cost	USD	0	31,960	31,960	59,898
Battery pack cost	USD	0	0	24,960	24,960
Annual electricity bill	USD	2,488	154	32	-1,746 (*)
Environmental balance					
Primary energy	TOE	5.991	0	0	-5.576 (*)
CO_2 emission (exp-imp)	kg	15,000	0	0	-13,950 (*)

(*) if the exportation of electricity surplus is possible

8. PassivHaus Certification and real building behavior

The PassivHaus certication represents, in temperate regions, the best award of energy savings in building design and the Passive House Planning Package (PHPP) is the tool used to verify the energy consumption of a building, according to a detailed building description. It has to be noted that PHPP calculations are based on a static evaluation linked to the monitored and numerically simulated population of existing passive houses [49]. Hence the PHPP energy evaluation can differ from the real behavior and from transient simulation especially in heavy external conditions and with variable internal loads, as considered in the present project of autonomous house.

As already mentioned, this building was certified by the PassivHaus and the PHPP certification reports a specific annual energy consumption for cooling production of 50 kWh/m^2a. However, it worth to be noted that the real consumption by field data (Table 9) and confirmed by Trnsys simulations resulted much higher, i.e. 67.8 kWh/m^2a. This significant difference can be easily explained by considering the following reasons:

1. different weather data;
2. different temperature set point (25 °C constant for PHPP);
3. random occurrence of internal loads for overload events (not predicted in the PHPP protocol).

9. Conclusions

The paper presents the very-first Energy+ building in Dubai certified by the Passive House Institute. The building is a pioneering autonomous house build up at the headquarter of the Mohammed Bin Rashid Space Center in Dubai. A measurement campaign has been carried out, by monitoring for one year the data from several sensors installed on the building envelope and in the energy plant. The design of the building was based on a scientific approach with extensive use of simulation tools. A Trnsys model of the building was developed to predict the energy demand for cooling and air dehumidification, by assuring a high level of comfort in every room. The energy plant consists on a 40 kW_p PV field, coupled to a 48 kWh battery storage and to a high-efficiency air-cooled electric chiller. It fulfills the energy demand, making the building energy-autonomous with a surplus of power production that is exported to the grid.

The simulation approach was also used to evaluate the over-sizing of the energy plants to reach the target of the full energy-autonomy. The PV field area is 87% higher than the surface required to meet the Net Zero Energy Building standard. The installed storage capacity is equivalent to the battery pack that allows to reduce the grid exchange from 32% to 10% of the total demand in the NZEB configuration.

After the first year of operation and data monitoring, the measurements confirm that the Trnsys model is very accurate and the predicted performance is in good agreement with the real data. This prototype has proved that a sustainable fully solar-powered building assuring a high level of comfort under the severe climate conditions of the Gulf area is an achievable target.

3. References

[1] P. Nejat, F. Jomehzadeh, M. M. Taheri, M. Gohari, M. Z. A. Majid, A global review of energy consumption, CO_2 emissions and policy in the residential sector (with an overview of the top ten CO_2 emitting countries), Renewable and sustainable energy reviews 43 (2015) 843-862.

[2] M. Thalfeldt, E. Pikas, J. Kurnitski, H. Voll, Façade design principles for nearly zero energy buildings in a cold climate, Energy and Buildings 67 (2013) 309-321.

[3] M. Justo Alonso, P. Liu, H. M. Mathisen, G. Ge, C, Simonson, Review of heat/energy recovery exchangers for use in ZEBs in cold climate countries, Building and Environment 84 (2015) 228-237.

[4] Y. Wang, J. Kulckelkorn, F. Zhao, H. Spliethoff, W. Lang, A state of art of review on interactions between energy performance and indoor environment quality in Passive House buildings, Renewable and Sustainable Energy Reviews 72 (2017) 1303-1319.

[5] E. Rodriguez-Ubinas, C. Montero, M. Porteros, S. Vega, I. Navarro, M. Castillo-Cagigal, E. Matallanas, A. Gutiérrez, Passive design strategies and performance of Net Energy Plus Houses, Energy and buildings 83 (2014) 10-22.

[6] M. Mihai, V. Tanasiev, C. Dinca, A. Badea, R. Vidu, Passive house analysis in terms of energy performance, Energy and buildings 144 (2017) 74-86.

[7] A. Krstić-Furundžić, T. Kosić, Assessment of energy and environmental performance of office building models: a case study, Energy and Buildings 115 (2016) 11-22.

[8] J. Schnieders, W. Feist, L. Rongen, Passive Houses for different climate zones, Energy and Buildings

105 (2015): 71-87.

[9] P. A. Fokaides, E. Christoforou, M. Ilic, A. Papadopoulos, Performance of a Passive House under subtropical climatic conditions, Energy and Buildings 133 (2016) 14-31.

[10] A. Juaidi, F. G. Montoya, J. A. Gázquez, F. Manzano-Agugliaro, An overview of energy balance compared to sustainable energy in United Arab Emirates, Renewable and Sustainable Energy Reviews 55 (2016) 1195-1209.

[11] Q. Roslan, S. Halipah Ibrahim, M. N. Mohd Nawi, A. Baharun, A literature review on the improvement strategies of passive design for the roofing system of the modern house in a hot and humid climate region, Frontiers of Architectural Research 5.1 (2016) 126-133.

[12] O. Irulegi, L. Torres, A. Serra, I. Mendizabal, R. Hernández, The Ekihouse: An energy self-sufficient house based on passive design strategies, Energy and Buildings 83 (2014) 57-69.

[13] W. A. Friess, K. Rakhshan, A review of passive envelope measures for improved building energy efficiency in the UAE, Renewable and Sustainable Energy Reviews 72 (2017) 485-496.

[14] M. Asif, Growth and sustainability trends in the buildings sector in the GCC region with particular reference to the KSA and UAE, Renewable and Sustainable Energy Reviews 55 (2016) 1267-1273.

[15] H. Taleb, M. A. Musleh, Applying urban parametric design optimisation processes to a hot climate: Case study of the UAE, Sustainable Cities and Society 14 (2015) 236-253.

[16] K. M. Al-Obaidi, M. Ismail, A. M. Abdul Rahman, Passive cooling techniques through reflective and radiative roofs in tropical houses in Southeast Asia: A literature review, Frontiers of Architectural Research 3.3 (2014) 283-297.

[17] A. K. Nanda, C. K. Panigrahi, A state-of-the-art review of solar passive building system for heating or cooling purpose, Frontiers in Energy 10.3 (2016) 347-354.

[18] F. A. Ghaith, R. Abusitta, Energy analyses of an integrated solar powered heating and cooling systems in UAE, Energy and Buildings 70 (2014) 117-126.

[19] B. J. Huang, T. F. Hou, P. C. Hsu, T. H. Lin, Y. T. Chen, C. W. Chen, K. Li, K. Y. Lee, Design of direct solar PV driven air conditioner, Renewable Energy 88 (2016) 95-101.

[20] R. M. Lazzarin, Solar cooling: PV or thermal? A thermodynamic and economical analysis, International Journal of Refrigeration 39 (2014) 38-47.

[21] A. AlAjmi, H. Abou-Ziyan, A. Ghoneim, Achieving annual and monthly net-zero energy of existing building in hot climate, Applied Energy 165 (2016) 511-521.

[22] C. Good, I. Andresen, A. G. Hestnes, Solar energy for net zero energy buildings–A comparison between solar thermal, PV and photovoltaic–thermal (PV/T) systems, Solar Energy 122 (2015) 986-996.

[23] M. Krarti, P. Ihm, Evaluation of net-zero energy residential buildings in the MENA region, Sustainable cities and society 22 (2016) 116-125.

[24] Z. Zhou, L. Feng, S. Zhang, C. Wang, G. Chen, T. Du, Y. Li, J. Zuo, The operational performance of "net zero energy building: A study in China, Applied energy 177 (2016) 716-728.

[25] S. Deng, R. Z. Wang, Y. J. Dai, How to evaluate performance of net zero energy building–A literature research, Energy 71 (2014) 1-16.

549 [26] A. J. Marszal, P. Heiselberg, J. S. Bourelle, E. Musall, K. Voss, I. Sartori, A. Napolitano, Zero Energy
550 Building–A review of definitions and calculation methodologies, Energy and buildings 43.4 (2011) 971-979.
551 [27] L. Fara, D. Craciunescu, Output analysis of stand-alone PV systems: modeling, simulation and
552 control, Energy Procedia 112 (2017) 595-605.
553 [28] E. Hoxha, T. Jusselme, On the necessity of improving the environmental impacts of furniture and
554 appliances in net-zero energy buildings, Science of The Total Environment 596 (2017) 405-416.
555 [29] V. S. K. V. Harish, A. Kumar, A review on modeling and simulation of building energy systems,
556 Renewable and Sustainable Energy Reviews 56 (2016) 1272-1292.
557 [30] M. Mihai, V. Tanasiev, C. Dinca, A. Badea, R. Vidu, Passive house analysis in terms of energy
558 performance, Energy and Buildings 144 (2017) 74-86.
559 [31] J. Widén, Improved photovoltaic self-consumption with appliance scheduling in 200 single-family
560 buildings, Applied Energy 126 (2014) 199-212.
561 [32] T. S. Blight, D. A. Coley, Sensitivity analysis of the effect of occupant behaviour on the energy
562 consumption of passive house dwellings, Energy and Buildings 66 (2013) 183-192.
563 [33] A. Satake, H. Ikegami, Y. Mitani, Energy-saving Operation and Optimization of Thermal Comfort
564 in Thermal Radiative Cooling/Heating System, Energy Procedia 100 (2016) 452-458.
565 [34] K. Zhao, X. H. Liu, Y. Jiang, Application of radiant floor cooling in large space buildings–A review,
566 Renewable and Sustainable Energy Reviews 55 (2016) 1083-1096.
567 [35] L. Pocero, D. Amaxilatis, G. Mylonas, I. Chatzigiannakis, Open source IoT meter devices for smart
568 and energy-efficient school buildings, HardwareX 1 (2017) 54-67.
569 [36] A. Erkoreka, E. Garcia, K. Martin, J. Teres-Zubiaga, L. Del Portillo, In-use office building energy
570 characterization through basic monitoring and modelling, Energy and Buildings 119 (2016) 256-266.
571 [37] O. Guerra-Santin, C. A. Tweed, In-use monitoring of buildings: An overview of data collection
572 methods, Energy and Buildings 93 (2015) 189-207.
573 [38] T. Babaei, H. Abdi, C. P. Lim, S. Nahavandi, A study and a directory of energy consumption data
574 sets of buildings, Energy and Buildings 94 (2015) 91-99.
575 [39] F. Ascione, N. Bianco, O. Böttcher, R. Kaltenbrunner, G. P. Vanoli, Net zero-energy buildings in
576 Germany: Design, model calibration and lessons learned from a case-study in Berlin, Energy and Buildings
577 133 (2016) 688-710.
578 [40] M. Royapoor, T. Roskilly, Building model calibration using energy and environmental data, Energy
579 and Buildings 94 (2015) 109-120.
580 [41] D. Coakley, P. Raftery, M. Keane, A review of methods to match building energy simulation models
581 to measured data, Renewable and sustainable energy reviews 37 (2014) 123-141.
582 [42] G. Mustafaraj, D. Marini, A. Costa, M. Keane, Model calibration for building energy efficiency
583 simulation, Applied Energy 130 (2014) 72-85.
584 [43] M. Jamil, A. Farzana, Y. J. Jeon, Renewable energy technologies adopted by the UAE: Prospects and
585 challenges–A comprehensive overview, Renewable and Sustainable Energy Reviews 55 (2016) 1181-1194.
586 [44] M. A. H. Mondal, S. Kennedy, T. Mezher, Long-term optimization of United Arab Emirates energy

587 future: policy implications, Applied Energy 114 (2014) 466-474.
588 [45] J. Al-Amir, B. Abu-Hijleh, Strategies and policies from promoting the use of renewable energy
589 resource in the UAE, Renewable and Sustainable Energy Reviews 26 (2013) 660-667.
590 [46] S. Sgouridis, A. Abdullah, S. Griffiths, D. Saygin, N. Wagner, D. Gielen, H. Reinisch, D. McQueen,
591 RE-mapping the UAE's energy transition: An economy-wide assessment of renewable energy options and
592 their policy implications, Renewable and Sustainable Energy Reviews 55 (2016) 1166-1180.
593 [47] G. Brumana, G. Franchini, A. Perdichizzi, Design and Performance Prediction of an Energy+
594 Building in Dubai, Energy Procedia 126 (2017) 155-162.
595 [48] Electronic resource. Indicators, Energy Efficiency. "Indicators by Country/Region 1990-2013 /World
596 Energy Council, 2015." Mode of access: https://wec-indicators.enerdata.net/secteur.php#/power-generation-
597 efficiency.html.
598 [49] Research Group for Cost-effective Passive Houses. Energy balances with the Passive House Planning
599 Package, Protocol Volume No. 13 of the, first edition, Passive House Institute, Darmstadt (1998).